

Article

Determination of Wax Deposition Rate Model of Blended Oils with Different Blending Ratios

Zhuo Han ¹, Lihui Ma ¹, Xiaowei Li ^{2,*}, Haoran Zhu ^{2,*}, Wei Li ¹, Xiaohang Xia ³, Xiaohan Zhang ¹ and Rui Guo ¹

¹ Technical Inspection Center, Sinopec Shengli Oilfield Company, Dongying 257000, China; hanzhuo.slyt@sinopec.com (Z.H.); malihui1128@163.com (L.M.); liwei027.slyt@sinopec.com (W.L.); zhangxh629.slyt@sinopec.com (X.Z.)

² School of Petroleum and Natural Gas Engineering, Changzhou University, Changzhou 213164, China

³ CNOOC Energy Technology & Services Limited, Beijing 100027, China; xiaxh4@cnooc.com.cn

* Correspondence: mpflxw@cczu.edu.cn (X.L.); zhuhaoran@cczu.edu.cn (H.Z.)

Abstract: Blending with light oil is a commonly used and reliable method of crude oil transportation, and the blending ratio is a crucial operating parameter in determining the safe and efficient operation of the pipeline. In this paper, in-house flow and deposition experiments are used to evaluate the flow and deposition characteristics of crude oils with varying blending ratios. The results show that (1) blending with light oil basically does not affect the shape of the DSC curve of crude oil; (2) blending with light oil will not eliminate the thermal treatment effect, and the mixed oil flowability still remains highly dependent on the thermal treatment temperature; (3) blending with light oil can greatly decrease the abnormal point and oil viscosity, in which the low-temperature viscosity decreases more significantly; and (4) a wax deposition model of mixed oil is obtained through the fitting of Huang's model, where the blending ratio is a crucial factor in the determination of the model parameters k , m , and n .

Keywords: blending ratio; waxy crude oil; flowability; wax deposition; model



Citation: Han, Z.; Ma, L.; Li, X.; Zhu, H.; Li, W.; Xia, X.; Zhang, X.; Guo, R. Determination of Wax Deposition Rate Model of Blended Oils with Different Blending Ratios. *Processes* **2024**, *12*, 772. <https://doi.org/10.3390/pr12040772>

Academic Editor: Blaž Likozar

Received: 13 March 2024

Revised: 10 April 2024

Accepted: 10 April 2024

Published: 11 April 2024



Copyright: © 2024 by the authors. Licensee MDPI, Basel, Switzerland. This article is an open access article distributed under the terms and conditions of the Creative Commons Attribution (CC BY) license (<https://creativecommons.org/licenses/by/4.0/>).

1. Introduction

Waxy crude oil is characterized by its large amount of paraffin wax molecules. It is an important type of fossil energy resource and is widespread in major oil fields around the world [1,2]. The wax molecules will undergo wax crystal precipitation and formation when the temperature reaches the wax appearance temperature (WAT) [3]. The formed solid particles lead to expansion of the contact area between the solid and liquid phases, thus increasing the oil viscosity. Furthermore, the precipitated wax crystal particles also have a tendency to accumulate on the pipe wall, reducing the flow area of the pipe and ultimately leading to increased frictional resistance within the pipeline [4,5].

To improve the oil's rheological characteristics and ensure reliable and cost-effective crude oil transportation, a series of methods (such as thermal treatment, adding pour point depressant, blending with light oil, sequential transportation, or a combination of various transportation methods) have been presented [6–12]. Among them, blending with light oil is a commonly used and reliable method. This method involves blending light crude oil with high-wax oil to enhance the oil flowability. However, the blending ratio often varies due to the inhomogeneity of on-site oil products in terms of type and quantity. The flowability of the blended crude oil is unclear, and the wax deposition characteristics are yet to be explored, which will lead to potential problems such as the severe wax deposition phenomenon, increased pipeline friction, etc. Therefore, it is necessary to conduct a systematic and in-depth study on the flow and deposition characteristics of crude oils with different blending ratios.

Regarding the prediction of rheological properties for mixtures of light and heavy crude oil, researchers have primarily focused on predicting the viscosity and pour point of

the blended oil. In most cases, the viscosity of the mixture cannot be obtained by simply adding the viscosity values of the individual component oils. The majority of calculation models for blended crude oil viscosity are empirical models, such as the Arrhenius model, Kendall–Monroe model, Bingham model, and Cragoe model [13–16]. Jing et al. [17] compared the effectiveness of four different models, including the Lederer model, Arrhenius model, double logarithmic model, and Cragoe model, to predict viscosity based on experimental viscosity data. The Cragoe model produced the smallest average relative error. Gao et al. [18] pointed out that the current models for predicting viscosity are limited and all of them are empirical models. To address this issue, the authors suggest the use of machine learning methods for viscosity prediction.

The pour point is a key parameter that reflects the oil's rheological characteristics. It is important to note that there is typically no simple additive relationship between pour points of different component oils [19]. Generally speaking, the pour point of a blended crude oil can be estimated as a weighted average of the pour points of its individual components. The wax content of blended crude oil can be estimated as a weighted average of the wax content of each component oil, and changes in the wax content will have a direct impact on wax precipitation and gelation processes. Furthermore, some studies have pointed out that mixing crude oils will cause a change in the state of asphaltene accumulation in crude oil. During the cooling process of crude oil, asphaltenes have complex nuclei and eutectic interactions with wax molecules [20]. Lei et al. [21,22] provided insights into the interaction between asphaltene and wax molecules by analyzing the microscopic morphology of wax crystals. They noted that the aggregation state of asphaltene can influence the fractal dimension and the microscopic properties of wax crystals. Zhu et al. [23,24] suggested that the temperature used for thermal treatment can alter the aggregation state of asphaltenes, causing changes in their flow characteristics and wax deposition. It is worth noting that waxy crude oils are known to exhibit thermal treatment effects, whereby the rheological properties of the oil at low temperatures can vary depending on the thermal treatment temperature. However, there are limited studies available in the literature concerning the effects of thermal treatment on mixed crude oils.

Scholars have previously proposed various mechanisms, such as molecular diffusion, aging and gelation, to explain oil wax deposition properties [25–27]. The effects of operating parameters [28,29] on wax deposition have been studied in detail, and wax deposition dynamic models have been established according to molecular diffusion and aging mechanisms [30–32]. However, the wax deposition characteristics of blended crude oils have not been thoroughly researched. The pour point and viscosity of mixed crude oils are typically influenced by the blending ratio as well as the properties of the component oils. Consequently, evaluating the wax deposition characteristics of blended crude oils poses a significant challenge for oil pipelines. However, there is currently a lack of effective prediction models for predicting the wax deposition rate of mixed crude oil, which leads to difficulties in predicting the wax deposition rate of mixed crude oil on site. Therefore, developing a wax deposition rate prediction model for mixed crude oil is of great significance in guiding the determination of on-site mixing proportions, the design of oil pipelines, and the determination of pigging cycles and plans. Huang's model was successfully adopted in the prediction of wax deposition rate [33,34], and in this paper, the aim is to propose a set of methods for predicting wax deposition rate, and obtain the parameters of the model based on Huang's model.

To investigate the effect of blending ratio on the properties of crude oil, we initially blended Shengli waxy crude oil and Saudi light crude oil at varying ratios to prepare different oil samples. Subsequently, we used DSC, a rheometer, and a Couette wax deposition experiment to evaluate the wax precipitation characteristics, flowability, pour point, and wax deposition of these samples. To analyze the impact of blending ratio on the flowability and wax deposition properties, we utilized parameters such as the WAT, viscosity, pour point, and wax deposition as the model variables. Ultimately, we obtained

the wax deposition rate models of different oil samples by fitting the experimental data, and analyzed the variation patterns of the model parameters with the blending ratio.

2. Materials and Methods

2.1. Crude Oil Sample

In this study, we considered two different types of crude oils: Shengli and Saudi crude oil. Shengli crude oil, with a wax appearance temperature (WAT) of 51 °C and wax content of 14.5 wt%, exhibits a high degree of waxiness and has a density of 897.5 g/cm³ at 20 °C. Hence, it can be regarded as a high-wax crude oil. On the other hand, Saudi crude oil has relatively lower WAT and wax content, thereby belonging to the class of light crude oils. The pure Shengli crude oil was labeled oil sample 1, while oil samples 2, 3, 4, and 5 were produced by blending Shengli and Saudi crude oil in different volume ratios (7:1, 6:2, 5:3, and 4:4). Generally speaking, the blending ratio of waxy crude oil and light oil is determined by the design output of the two crude oils on site. In this paper, we want to study the influence of blending ratio on wax deposition characteristics. Therefore, the specific blending ratio is mainly Shengli waxy crude oil blended with a smaller amount of Saudi light crude oil.

2.2. Methods

2.2.1. DSC Test

The wax precipitation characteristics of oil samples with different blending ratios were analyzed using a DSC 821e differential scanning calorimeter. The test sample was added into a crucible and heated to 80 °C for 5 min to completely melt the wax crystal particles. Then, the oil sample was cooled to −25 °C at a constant cooling rate of 5 °C/min. The wax appearance temperature (WAT) and wax content of the oil sample at −20 °C can be identified and calculated according to the obtained DSC curve [23,24].

2.2.2. Pour Point Test

We evaluated the pour points of oil samples with different blending ratios. Initially, each oil sample was heated to its respective thermal treatment temperature (i.e., 50, 60, 70, 80 °C) and left undisturbed for an hour to eliminate any complex thermal and shear history effects. Subsequently, the oil sample was placed into a test tube and cooled at a cooling rate of 0.5–1 °C/min. When the oil temperature decreased to 8 °C above the estimated pour point, the oil sample was examined every 2 °C. The pour point was determined as the temperature at which the test tube was tilted horizontally and maintained in that position for 5 s without any oil sample flowing.

2.2.3. Rheological Test

Initially, the oil sample was heated to 80 °C and this temperature maintained for an hour to ensure complete melting of the wax crystal particles. Subsequently, the oil sample was sent to the rheometer (TA, New Castle, DE, USA) and the oil temperature was decreased, while applying shear rates of 10, 21.5, 46.4, 100, and 200 s^{−1} during the cooling process. The oil viscosity under these conditions was recorded at a steady state.

2.2.4. Wax Deposition Experiment

To determine the wax deposition properties of different oil samples, the Couette wax deposition experimental device was adopted. This device has been described in detail in previous papers [35,36]. As displayed in Figure 1, the Couette wax deposition experimental device is mainly composed of a hot bath, a cold bath, a torque sensor, a lifter, a sample barrel ($R_1 = 52$ mm), a wax deposition barrel ($R_2 = 25.5$ mm), and a conveyor. In a wax deposition test, the sample barrel rotates at a fixed rotating speed, while the inner wax deposition barrel is stationary. Initially, the oil sample was heated to a thermal treatment temperature of 80 °C and left to stabilize for an hour. Subsequently, the oil temperature was reduced at a cooling rate of 0.5–1 °C/min. As soon as the oil temperature reached its

corresponding temperature, it was added to the oil sample barrel. Next, the wax deposition barrel, maintained at a fixed temperature, was introduced into the crude oil, and the wax deposition experiment commenced. Meanwhile, the rotation barrel was turned consistently at a predetermined speed (50, 100, or 150 r/min). After completing the wax deposition experiment, we calculated the deposition rate and utilized the wax deposition model developed by Huang et al. [33,34] to fit the measured deposition rates.

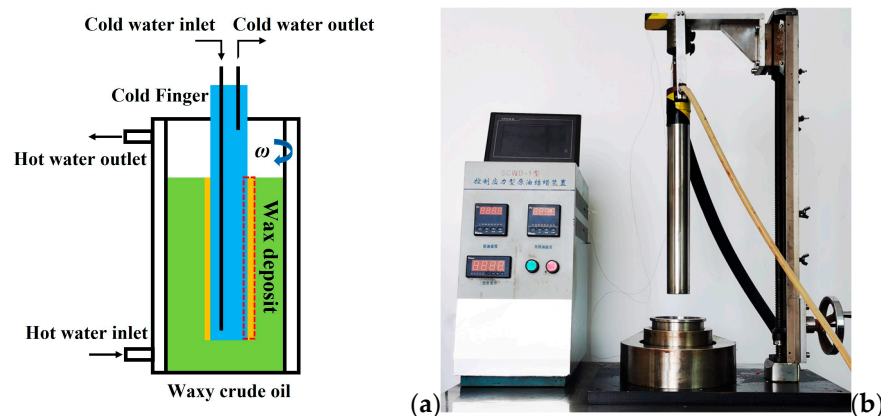


Figure 1. Couette wax deposition experimental device. (a) Schematic diagram; (b) physical map.

3. Results

3.1. Thermal Physical Parameters of Blended Oil

The wax precipitation characteristics of oil samples 1–5 are displayed in Figure 2. As displayed in Figure 2a, the DSC curve of the pure Shengli crude oil (oil sample 1) exhibits two distinct wax precipitation peaks. The first peak is relatively small and appears in the temperature range of 40–50 °C, while the second and larger peak occurs within the temperature range of –20–40 °C. The WAT and wax content are important thermal physical parameters, and directly determine the flow and deposition behavior. The WAT can be identified as the first temperature at which heat flow increases during the temperature drop in the DSC curve. The determination of WAT for pure Shengli crude oil results in a value of 51 °C, and oil sample 1 accumulates a wax content of 14.5 wt% at –20 °C.

As shown in Figure 2b–e, the shapes of the DSC curve for oil samples 2–5 remain constant even as the blending ratio increases. Furthermore, both the small and the large wax precipitation peaks are still observable. However, the WAT and accumulated precipitated wax contents of crude oil gradually decrease as the blending ratio increases. At a blending ratio of 87.5%, the WAT and wax content of oil sample 2 decrease to 48 °C and 12.8 wt%, respectively (Figure 3a,b). Subsequently, with a continuous increase in the blending ratio to 75%, 62.5%, and 50%, there is a gradual decrease in the WAT and wax content of the crude oil, with values of 46 °C/11.1 wt%, 43 °C/10.4 wt%, and 40 °C/8.4 wt%, respectively. The WAT and wax content of crude oil are strongly linearly related to the blending ratio. The R2 values of the fitted equations in Figure 3a,b are 0.996 and 0.984, respectively. Thus, we can easily obtain the WAT and wax content through the fitted equations in Figure 3a,b.

The wax crystal solubility coefficients of crude oils with varying blending ratios are displayed in Figure 3c. The values of the wax crystal solubility coefficients vary with the oil sample temperature. In addition, the solubility coefficient of wax crystals progressively decreases as the blending ratio increases. For example, the wax crystal solubility coefficients of oil samples 1–5 at 30 °C are 0.27, 0.14, 0.14, 0.05, and 0.03 °C⁻¹, respectively.

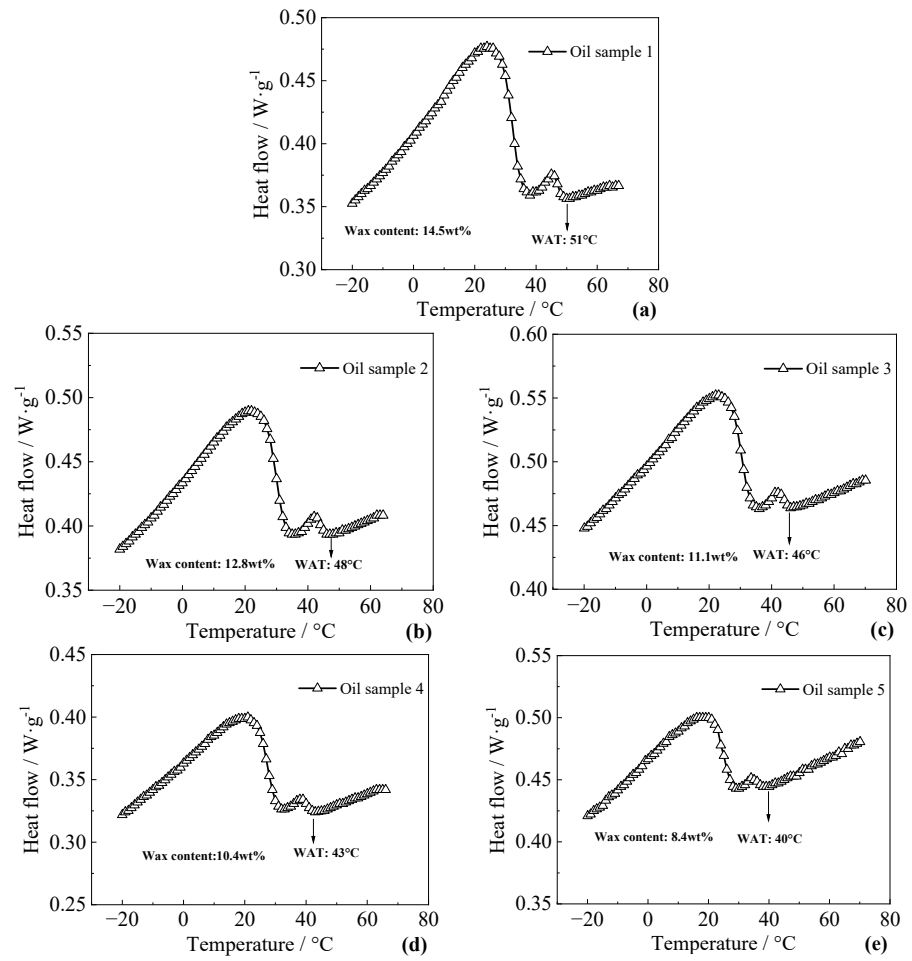


Figure 2. WAT and wax content of crude oils with different blending ratios. (a) 100%; (b) 87.5%; (c) 75%; (d) 62.5%; (e) 50%.

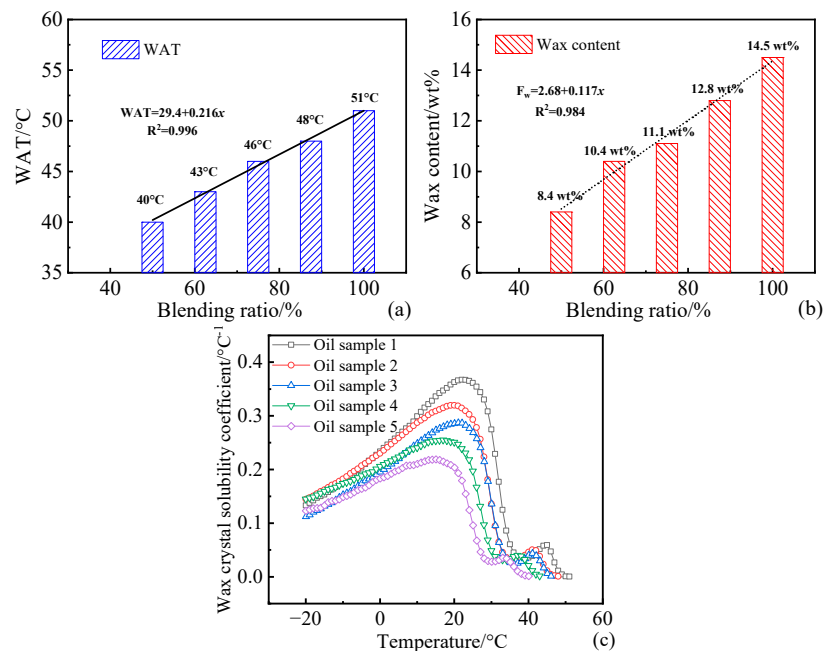


Figure 3. Thermal physical parameters of crude oils with different blending ratios. (a) WAT; (b) wax content; (c) wax crystal solubility coefficient.

3.2. Flow Characteristic Parameters of Blended Oil

The flow characteristics of crude oils with varying blending ratios are illustrated in Figure 4. The pure Shengli oil has an abnormal point of 37 °C. The viscosity remains consistent at different shear rates at temperatures higher than 37 °C. As the temperature decreases, the viscosity increases slowly, indicating that there is either no wax crystal precipitation or the amount of wax crystal precipitated is too small to cause the deterioration of crude oil flowability. However, a sharp increase in viscosity is observed below 37 °C. Moreover, the crude oil exhibits strong shear-thinning behavior.

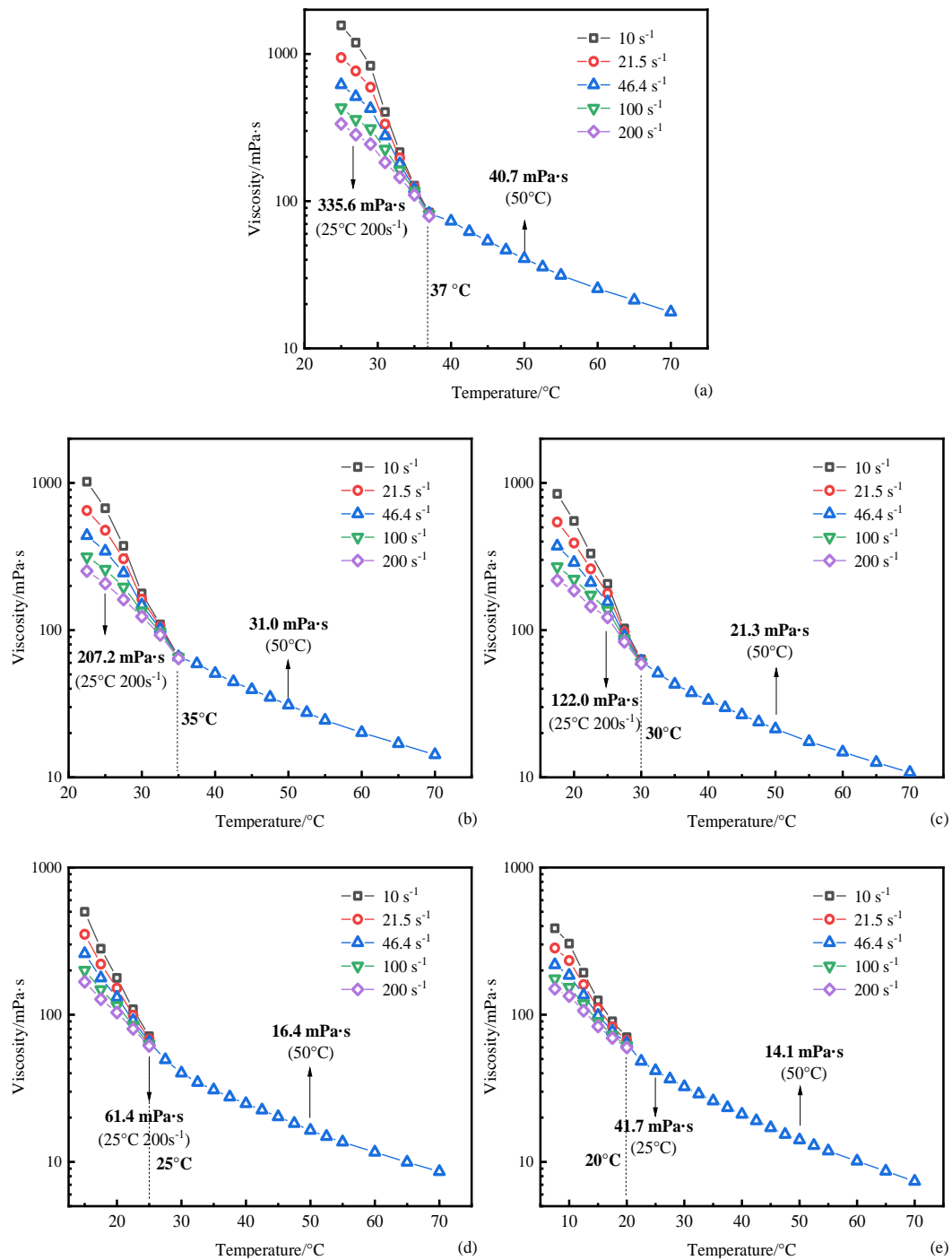


Figure 4. Flow curves of crude oils with different blending ratios. (a) 100%; (b) 87.5%; (c) 75%; (d) 62.5%; (e) 50%.

The oil viscosity at different temperatures gradually decreases as the blending ratio increases. For example, as displayed in Figure 5a, the viscosities of oil samples 1–5 at 50 °C are 40.7, 31.0, 21.3, 16.4, and 14.1 mPa·s, respectively. Moreover, the apparent viscosities of oil samples 1–5 at 25 °C under a shear rate of 200 s⁻¹ are 335.6, 207.2, 122.0, 61.4, and 41.7 mPa·s. We found that lighter oil products can decrease the oil viscosity, and in regions with high temperatures that are above the WAT, light oil products will dilute the waxy crude oil. At oil temperatures below the WAT, increasing the blending ratio will decrease the oil viscosity, and the precipitated wax crystal amount will also decrease (as shown in Figure 2), which further leads to a decrease in oil viscosity. Therefore, as illustrated in Figure 5b, the abnormal point gradually decreases from 37 °C for oil sample 1 to 35, 30, 25, and 20 °C under blending ratios of 87.5%, 75%, 62.5%, and 50%.

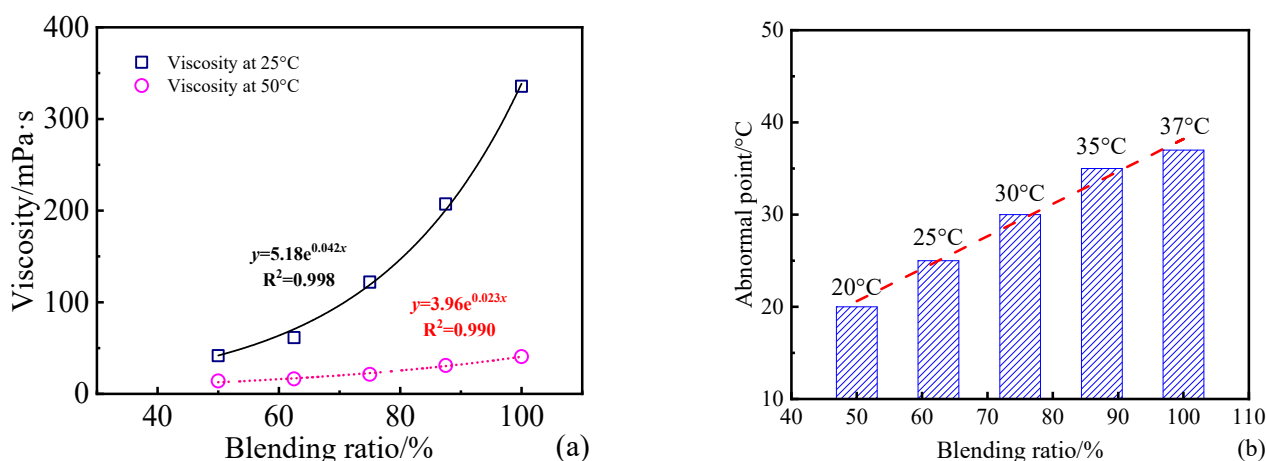


Figure 5. Viscosity and abnormal point of crude oil under different blending ratios. (a) Viscosity; (b) abnormal point.

3.3. Gelation Behavior of Blended Oil

Table 1 demonstrates the pour points of oil samples at different thermal treatment temperatures. The pour points of oil samples 1–5 exhibit a strong correlation with the thermal treatment temperature. Take oil sample 1 (pure Shengli crude oil) as an example; the pour point at the thermal treatment temperature of 50 °C is 30 °C. As the thermal treatment temperature is raised to 60 °C and subsequently to 70 and 80 °C, there is a progressive reduction in the pour point, with the values decreasing to 28, 27, and 24 °C, respectively.

Table 1. Pour points of oil samples at different thermal treatment temperatures.

Thermal Treatment Temperature/°C	50	60	70	80
Oil sample 1	30	28	27	24
Oil sample 2	27	25	24	23
Oil sample 3	24	21	20	19
Oil sample 4	20	16	15	14
Oil sample 5	17	13	11	10

With a continuous increase in the blending ratio, the pour point of crude oil gradually decreases. For example, at a thermal treatment temperature of 80 °C, the pour points of oil samples 1–5 are 24, 23, 19, 14, and 10 °C. Remarkably, at a blending ratio of 50%, the pour point of oil sample 5 drops to less than half of that of oil sample 1. The same is true at thermal treatment temperatures of 50, 60, and 70 °C. Furthermore, we also found that for the Shengli waxy crude oil, blending light crude oil will not affect its thermal treatment effect. There is still a strong linear relationship between the pour point and the blending ratio.

3.4. Wax Deposition Characteristics of Blended Oil

The wax deposition properties of pure Shengli waxy crude oil are presented in Table 2, while those of oil samples 2–5 are detailed in Supplementary Tables S1–S4, which can be found in the supporting information. As illustrated in Table 2, the wall shear stress and the temperature gradient are calculated through the steady state calculation of Fluent software (version number: 2021R2). The wax crystal solubility coefficient and oil viscosity can be obtained from Figures 2 and 4. The deposition rate was fitted using the model presented by Huang et al. [34] (Equation (1)), and the obtained wax deposition models are expressed in Table 3.

$$W = k\tau^m \frac{1}{\mu} \frac{dC}{dT} \frac{dT}{dr}^n \quad (1)$$

where W refers to the wax deposition rate, $\text{g}\cdot\text{m}^{-2}\cdot\text{h}^{-1}$; τ refers to the wall shear stress, Pa; μ is the oil viscosity at the pipe wall, Pa·s; dC/dT is the wax crystal solubility coefficient, $1/^\circ\text{C}$; dT/dr is the temperature gradient, $^\circ\text{C}\cdot\text{m}^{-1}$; and k , m , and n are the fitting parameters of the wax deposition model.

Table 2. Wax deposition characteristics of oil sample 1.

Oil Temperature / $^\circ\text{C}$	Wall Temperature / $^\circ\text{C}$	Rotation Speed /($\text{r}\cdot\text{min}^{-1}$)	Wall Shear Stress /Pa	Oil Viscosity /Pa·s	Wax Crystal Solubility Coefficient $\times 10^{-4}/^\circ\text{C}$	Temperature Gradient / $^\circ\text{C}\cdot\text{m}^{-1}$	Wax Deposition Rate / $\text{g}\cdot\text{m}^{-2}\cdot\text{h}^{-1}$
42	32	150	3.576	0.207	17.70	579.0	9.14
45	35	150	2.717	0.127	6.07	578.8	4.96
48	38	150	2.246	0.088	3.47	578.9	5.56
51	41	150	1.885	0.068	3.88	576.8	7.89
55	45	150	1.508	0.054	5.93	574.3	16.26
58	48	150	1.291	0.046	1.15	573.6	4.01
37	32	150	4.874	0.193	17.70	291.4	5.21
47	32	150	2.847	0.217	17.70	867.6	10.55
52	32	150	2.329	0.226	17.70	1152.0	12.25
50	45	150	1.757	0.054	5.93	288.4	11.33
60	45	150	1.317	0.054	5.93	859.3	24.22
65	45	150	1.167	0.054	5.93	1143.0	25.44
55	45	50	0.503	0.054	5.93	574.3	29.75
55	45	100	1.005	0.054	5.93	574.3	19.93
42	32	50	1.231	0.272	17.7	579.0	12.10
42	32	100	2.414	0.229	17.7	579.0	9.98

Table 3. Wax deposition models of oil samples 1–5.

Oil Sample	Wax Deposition Model
Oil sample 1	$W = 105.3538\tau_w^{-0.531} \frac{1}{\mu} \frac{dC}{dT} \left(\frac{dT}{dr}\right)^{0.457}$
Oil sample 2	$W = 83.1534\tau_w^{-0.5652} \frac{1}{\mu} \frac{dC}{dT} \left(\frac{dT}{dr}\right)^{0.417}$
Oil sample 3	$W = 73.1272\tau_w^{-0.6106} \frac{1}{\mu} \frac{dC}{dT} \left(\frac{dT}{dr}\right)^{0.3926}$
Oil sample 4	$W = 54.1652\tau_w^{-0.698} \frac{1}{\mu} \frac{dC}{dT} \left(\frac{dT}{dr}\right)^{0.349}$
Oil sample 5	$W = 42.493\tau_w^{-0.767} \frac{1}{\mu} \frac{dC}{dT} \left(\frac{dT}{dr}\right)^{0.319}$

As the blending ratio continues to increase, the parameters of the wax deposition model also undergo significant changes. To illustrate this, Table 3 highlights the wax deposition models of crude oil at varying blending ratios.

As shown in Table 3, as the blending ratio increases, the parameters k , m , and n change accordingly. The parameter k decreases continuously, which shows to a certain extent that

increasing the mixing ratio is beneficial to reduce the deposition rate. An increase in the blending ratio is beneficial to reducing the wax deposition rate. The absolute value of the parameter m increases gradually with an increase in the blending ratio, while n gradually decreases with an increase in the blending ratio, indicating that as the sensitivity of the wax deposition rate to the shear stress of the pipe wall increases, the sensitivity to temperature gradients is weakened (Figure 6).

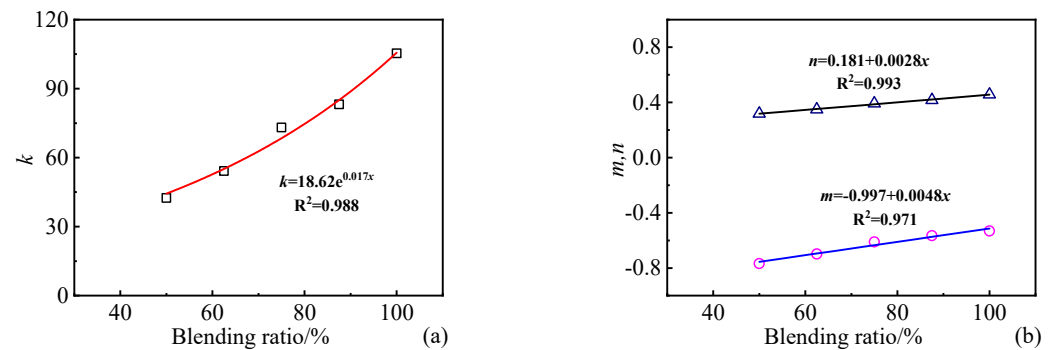


Figure 6. Relationship between wax deposition model parameters k , m , and n and the blending ratio. (a) k ; (b) m and n .

The relationships between parameters k , m , and n and the blending ratio are shown in Equations (2)–(4); the fitting accuracies of Equations (2)–(4) are 0.988, 0.971, and 0.993, respectively, indicating that the rate of wax deposition can be obtained through the model presented by Huang et al. [34] once we obtain the blending ratio.

$$k = 18.62e^{0.017x} \quad (2)$$

$$m = -0.997 + 0.0048x \quad (3)$$

$$n = 0.181 + 0.0028x \quad (4)$$

where x refers to the blending ratio, %, and k , m , and n are the parameters of the wax deposition model.

3.5. Discussion on the Flowability and Wax Deposition Characteristics of Blended Oils

As detailed from Sections 3.1–3.4, we can conclude that blending light crude oil into waxy crude oil is an effective way to improve the flowability and wax deposition characteristics of waxy crude oil. That is, with an increase in the blending ratio of light waxy crude oil, the WAT and wax content of blending oil gradually decrease. The changing rate follows a very good linear relationship. We realized that the blending operation only changed the composition of the crude oil without other obvious chemical changes. Thus, the flowability (including apparent viscosity, abnormal point, and pour point) of blended oil can be improved. Similarly, we can obtain the flow characteristics of crude oil with any blending ratio through curve fitting. Moreover, we obtained the wax deposition characteristics of five crude oils through wax deposition experiments and fitted the wax deposition model parameters based on Huang's model. We found that the model parameters are closely related to the blending ratio, and finally obtained the wax deposition model parameter of blending oils with different blending ratios.

The series of prediction methods proposed in this article for flow and wax deposition characteristic can be used in the design and operation management of crude oil blending transportation pipelines. For example, in the design stage of oil pipelines, the blending ratio range can be reasonably determined based on the amounts of waxy crude oil and light crude oil, and the economics of pipeline transportation can be evaluated based on this blending ratio range to optimize the most economical blending ratio. For oil pipelines that are already in operation, it is necessary to adjust the temperature conditions in and out

of the station in real time based on the dynamic changes in the blending ratio, and at the same time, predict the distribution of wax deposition in the pipeline, so as to reasonably determine the pigging cycle.

4. Conclusions

In this paper, we presented a comprehensive study on the determination of wax deposition rate models for blended oils with varying blending ratios and conducted an extensive series of experiments to evaluate the flow and deposition characteristics of crude oils blended in different ratios, focusing on parameters like wax appearance temperature (WAT), viscosity, pour point, and wax content. We obtained the following main conclusions:

- (1) An increase in the blending ratio does not change the shape of the DSC curves, while the WAT and wax content of crude oil linearly decrease.
- (2) With an increase in the blending ratio, the oil viscosity and abnormal point decrease, which shows that the crude oil flowability improves macroscopically.
- (3) The thermal treatment effect still exists in the blended crude oil, and the rheological properties of the blended crude oil gradually improve with an increase in the thermal treatment temperature.
- (4) With an increase in the blending ratio of crude oil, the wax deposition rate model parameters of crude oil gradually change. k gradually decreases, indicating that the wax deposition rate shows a decreasing trend. The absolute value of m increases gradually, and the value of n decreases gradually, indicating that the sensitivity of the wax deposition rate to the shear stress of the pipe wall increases, and the sensitivity to temperature gradient decreases.

The wax deposition rate prediction model proposed in this article can be used for the design, dynamic operation adjustment, and wax removal cycle determination of blended crude oil pipelines.

Supplementary Materials: The following supporting information can be downloaded at: <https://www.mdpi.com/article/10.3390/pr12040772/s1>, Table S1: Wax deposition characteristics of oil sample 2; Table S2: Wax deposition characteristics of oil sample 3; Table S3: Wax deposition characteristics of oil sample 4; Table S4: Wax deposition characteristics of oil sample 5.

Author Contributions: Methodology, Z.H., W.L. and L.M.; software, X.L. and H.Z.; validation, X.X.; investigation, X.Z. and R.G. All authors have read and agreed to the published version of the manuscript.

Funding: This research was funded by Jiangsu Key Laboratory of Oil and Gas Storage and Transportation Technology (grant number CDYQCY202204, CDYQCY202203).

Data Availability Statement: The data are contained within the article or Supplementary Materials.

Conflicts of Interest: Z.H., L.M., W.L., X.Z. and R.G. are employed by the Sinopec Shengli Oilfield Company. The author X.X. is employed by the company CNOOC Energy Technology & Services Limited. The remaining authors declare that this research was conducted in the absence of any commercial or financial relationships that could be construed as potential conflicts of interest.

References

1. Alnaimat, F.; Ziauddin, M. Wax deposition and prediction in petroleum pipelines. *J. Pet. Sci. Eng.* **2020**, *184*, 106385. [[CrossRef](#)]
2. Liu, Z.; Li, Y.; Wang, W.; Song, G.; Lu, Z.; Ning, Y. Wax and wax-hydrate deposition characteristics in single-, two-, and three-phase pipelines: A review. *Energy Fuels* **2020**, *34*, 13350–13368. [[CrossRef](#)]
3. Ruwoldt, J.; Kurniawan, M.; Oschmann, H. Non-linear dependency of wax appearance temperature on cooling rate. *J. Pet. Sci. Eng.* **2018**, *165*, 114–126. [[CrossRef](#)]
4. Van der Geest, C.; Melchuna, A.; Bizarre, L.; Bannwart, A.C.; Guersoni, V.C. Critical review on wax deposition in single-phase flow. *Fuel* **2021**, *293*, 120358. [[CrossRef](#)]
5. Visintin, R.F.; Lapasin, R.; Vignati, E.; D'Antona, P.; Lockhart, T.P. Rheological behavior and structural interpretation of waxy crude oil gels. *Langmuir* **2005**, *21*, 6240–6249. [[CrossRef](#)]
6. Zhu, H.; Lei, Y.; Li, C.; Yao, B.; Yang, F.; Li, S.; Peng, H.; Yu, P. Experimental and mechanism investigation on flowability and wax deposition of waxy crude oil with dissolved CH₄ by pressurized laboratory apparatus. *Fuel* **2023**, *343*, 127907. [[CrossRef](#)]

7. Yang, F.; Zhao, Y.; Sjöblom, J.; Li, C.; Paso, K.G. Polymeric wax inhibitors and pour point depressants for waxy crude oils: A critical review. *J. Dispers. Sci. Technol.* **2015**, *36*, 213–225. [[CrossRef](#)]
8. Martínez-Narro, G.; Pozos-Vázquez, C.; Núñez-Delgado, A.; Morán-Medellín, D.; Lara-Zárate, V.E. Heavy crude oil viscosity reduction by dilution with hydrocarbons obtained via pyrolysis of polypropylene and polystyrene. *Pet. Sci. Technol.* **2020**, *38*, 651–658. [[CrossRef](#)]
9. Ding, J.; Liu, D.; Tang, S.; Ren, S.; Yu, H. Study on temperature field reconstruction of cold and hot crude oil transportation. *J. Liaoning Univ. Pet. Chem. Technol.* **2017**, *37*, 34.
10. Yao, B.; Li, C.; Yang, F.; Sun, G.; Xia, X.; Ashmawy, A.M.; Zeng, H. Advances in and Perspectives on Strategies for Improving the Flowability of Waxy Oils. *Energy Fuels* **2022**, *36*, 7987–8025. [[CrossRef](#)]
11. Al-Mishaal, O.F.; Suwaid, M.A.; Al-Muntaser, A.A.; Khelkhal, M.A.; Varfolomeev, M.A.; Djimasbe, R.; Zairov, R.R.; Saeed, S.A.; Vorotnikova, N.A.; Shestopalov, M.A.; et al. Octahedral cluster complex of molybdenum as oil-soluble catalyst for improving in situ upgrading of heavy crude oil: Synthesis and application. *Catalysts* **2022**, *12*, 1125. [[CrossRef](#)]
12. Tajik, A.; Farhadian, A.; Khelkhal, M.A.; Rezaeisadat, M.; Petrov, S.M.; Eskin, A.A.; Vakhin, A.V.; Golafshani, M.B.; Lapuk, S.E.; Buzurov, A.E.; et al. Sunflower oil as renewable biomass source to develop highly effective oil-soluble catalysts for in-situ combustion of heavy oil. *Chem. Eng. J.* **2023**, *453*, 139813. [[CrossRef](#)]
13. Liu, Y.; Shi, S.; Wang, Y.; Feng, Y.; Luo, C. Calculation of heavy oil viscosity based on an Arrhenius model. *Pet. Sci. Technol.* **2017**, *35*, 1196–1202. [[CrossRef](#)]
14. Mohammadi, S.; Sobati, M.A.; Sadeghi, M. Viscosity reduction of heavy crude oil by dilution methods: New correlations for the prediction of the kinematic viscosity of blends. *Iran. J. Oil Gas Sci. Technol.* **2019**, *8*, 60–77.
15. Ding, H.; Wang, C.; Zhu, X. Estimation of the kinematic viscosities of bio-oil/alcohol blends: Kinematic viscosity-temperature formula and mixing rules. *Fuel* **2019**, *254*, 115687. [[CrossRef](#)]
16. Hernández, E.A.; Sánchez-Reyna, G.; Ancheyta, J. Evaluation of mixing rules to predict viscosity of petrodiesel and biodiesel blends. *Fuel* **2021**, *283*, 118941. [[CrossRef](#)]
17. Jing, J.; Yin, R.; Yuan, Y.; Shi, Y.; Sun, J.; Zhang, M. Determination of the transportation limits of heavy crude oil using three combined methods of heating, water blending, and dilution. *ACS Omega* **2020**, *5*, 9870–9884. [[CrossRef](#)] [[PubMed](#)]
18. Gao, X.; Dong, P.; Cui, J.; Gao, Q. Prediction model for the viscosity of heavy oil diluted with light oil using machine learning techniques. *Energies* **2022**, *15*, 2297. [[CrossRef](#)]
19. Zhang, J.; Zhao, T.; Wu, H. *Addition of a Heavy Crude May Facilitate Pipelining of Some Waxy Crudes*; UNITAR: New York, NY, USA, 1995.
20. Yang, F.; Zhu, H.; Li, C.; Yao, B.; Wang, F.; Chen, J.; Sun, G. Investigation on the mechanism of wax deposition inhibition induced by asphaltenes and wax inhibitors. *J. Pet. Sci. Eng.* **2021**, *204*, 108723. [[CrossRef](#)]
21. Lei, Y.; Li, S.; Liu, X.; Wang, H.; Zhu, H.; Gao, Y.; Peng, H.; Yu, P. Effect of existence state of asphaltenes on microstructure of wax crystals: Fractal dimension and unit cell structure. *J. Mol. Liq.* **2022**, *365*, 120132. [[CrossRef](#)]
22. Lei, Y.; Yu, P.; Ni, W.; Peng, H.; Liu, Y.; Lv, X.; Zhao, H. Study on the kinetic process of asphaltene precipitation during crude oil mixing and its effect on the wax behavior of crude oil. *ACS Omega* **2021**, *6*, 1497–1504. [[CrossRef](#)]
23. Zhu, H.; Li, C.; Yang, F.; Liu, H.; Liu, D.; Sun, G.; Yao, B.; Liu, G.; Zhao, Y. Effect of thermal treatment temperature on the flowability and wax deposition characteristics of Changqing waxy crude oil. *Energy Fuels* **2018**, *32*, 10605–10615. [[CrossRef](#)]
24. Li, C.; Zhu, H.; Yang, F.; Liu, H.; Wang, F.; Sun, G.; Yao, B. Effect of asphaltene polarity on wax precipitation and deposition characteristics of waxy oils. *Energy Fuels* **2019**, *33*, 7225–7233. [[CrossRef](#)]
25. Yang, J.; Lu, Y.; Daraboina, N.; Sarica, C. Wax deposition mechanisms: Is the current description sufficient? *Fuel* **2020**, *275*, 117937. [[CrossRef](#)]
26. Huang, Z.; Zheng, S.; Fogler, H.S. *Wax Deposition: Experimental Characterizations, Theoretical Modeling, and Field Practices*; CRC Press: Boca Raton, FL, USA, 2016.
27. Mahir, L.H.A.; Vilas Bôas Fávero, C.; Ketjuntwiwa, T.; Fogler, H.S.; Larson, R.G. Mechanism of wax deposition on cold surfaces: Gelation and deposit aging. *Energy Fuels* **2018**, *33*, 3776–3786. [[CrossRef](#)]
28. Janamatti, A.; Lu, Y.; Ravichandran, S.; Sarica, C.; Daraboina, N. Influence of operating temperatures on long-duration wax deposition in flow lines. *J. Pet. Sci. Eng.* **2019**, *183*, 106373. [[CrossRef](#)]
29. Li, R.; Huang, Q.; Huo, F.; Fan, K.; Li, W.; Zhang, D. Effect of shear on the thickness of wax deposit under laminar flow regime. *J. Pet. Sci. Eng.* **2019**, *181*, 106212. [[CrossRef](#)]
30. Mahir, L.H.A.; Lee, J.; Fogler, H.S.; Larson, R.G. An experimentally validated heat and mass transfer model for wax deposition from flowing oil onto a cold surface. *AIChE J.* **2021**, *67*, e17063. [[CrossRef](#)]
31. Huang, Z.; Lee, H.S.; Senra, M.; Scott Fogler, H. A fundamental model of wax deposition in subsea oil pipelines. *AIChE J.* **2011**, *57*, 2955–2964. [[CrossRef](#)]
32. Li, R.; Huang, Q.; Zhang, D.; Zhu, X.; Shan, J.; Wang, J. An aging theory-based mathematic model for estimating the wax content of wax deposits using the Fick's second law. *AIChE J.* **2020**, *66*, e16892. [[CrossRef](#)]
33. Ji, Z.; Li, C.; Yang, F.; Cai, J.; Cheng, L.; Shi, Y. An experimental design approach for investigating and modeling wax deposition based on a new cylindrical Couette apparatus. *Pet. Sci. Technol.* **2016**, *34*, 570–577. [[CrossRef](#)]
34. Huang, Q.; Li, Y.; Zhang, J. Unified wax deposition model. *Acta Pet. Sin.* **2008**, *29*, 459. [[CrossRef](#)]

35. Li, C.; Cai, J.; Yang, F.; Zhang, Y.; Bai, F.; Ma, Y.; Yao, B. Effect of asphaltenes on the stratification phenomenon of wax-oil gel deposits formed in a new cylindrical Couette device. *J. Pet. Sci. Eng.* **2016**, *140*, 73–84. [[CrossRef](#)]
36. Yang, F.; Cheng, L.; Liu, H.; Yao, B.; Li, C.; Sun, G.; Zhao, Y. Comb-like polyoctadecyl acrylate (POA) wax inhibitor triggers the formation of heterogeneous waxy oil gel deposits in a cylindrical couette device. *Energy Fuels* **2018**, *32*, 373–383. [[CrossRef](#)]

Disclaimer/Publisher’s Note: The statements, opinions and data contained in all publications are solely those of the individual author(s) and contributor(s) and not of MDPI and/or the editor(s). MDPI and/or the editor(s) disclaim responsibility for any injury to people or property resulting from any ideas, methods, instructions or products referred to in the content.